

Cancer-Related Heterocyclic Compound and Target Protein Interactions

Vishal Bhavsar^{1*}, Neelu Jain²

¹Scholar, Department of Chemistry, Mansarovar Global University, Bhopal, M.P., India

²Professor, Department of Chemistry, Mansarovar Global University, Bhopal, M.P., India

Received: 17th Sep, 2024; Revised: 14th Oct, 2024; Accepted: 22nd Nov, 2024; Available Online: 25th Dec, 2024

ABSTRACT

Cancer is the second most deadly illness in the world. According to the World Health Organization, 22 million more cases of cancer would be reported globally by the year 2030. The world over, researchers are devoting a lot of time and energy to finding better ways to detect, prevent, and cure cancer. Because of epigenetic and genetic aberrations, cancer cells have a different metabolic profile than normal cells. Heterocycles are the main structural component of many anti-cancer drugs that are now available. Furthermore, heterocyclic rings are structural components of anticancer drugs that were approved by the FDA from 2010 to 2015. Their inclusion in anti-cancer drugs may be attributed to their large cellular processes and mechanisms as well as their abundance in nature. Several heterocyclic compounds with anticancer effects on different cell lines are highlighted in this research. The nitrogen, sulfur, and oxygen atoms in these rings give the compounds their unique structure. Data collected on heterocyclic rings may one day lead to the development of new drugs that help combat cancer.

Keywords: Heterocyclic compounds, Anticancer activity, Cell lines, Cytotoxicity, Natural product

How to cite this article: Vishal Bhavsar, Neelu Jain. Cancer-Related Heterocyclic Compound and Target Protein Interactions. International Journal of Pharmaceutical Quality Assurance. 2024;15(4):2794-98. doi: 10.25258/ijpqa.15.4.88

Source of support: Nil.

Conflict of interest: None

INTRODUCTION

Although most research has concentrated on VEGF as a starting point, various cancer targets have been identified, such as enzymes that deacetylate histones, tyrosine kinase, TGF- α , FGF, PGF, EGF, and phosphodiesterase type I and II. The effectiveness of suppressing VEGF signaling has been modest, and there have been instances of disease progression after medication. Researchers are always looking for new heterocyclic anticancer medications to add to the current list of those in use, which includes both synthetic and naturally occurring compounds. Figure 1 shows that there are a few of these cases. Heterocyclic compounds have been studied for their potential medicinal uses in treating cancer and other diseases. These compounds are ring-shaped and include carbon with one or more nitrogen, oxygen, or sulfur atoms. By enhancing their solubility, polarity, and hydrogen bonding capabilities, these heteroatoms optimize druggable possibilities for ADMET (Adsorption, Distribution, Metabolism, Excretion, and Toxicity).

Brevilin A, commonly known as is an anticancer natural chemical obtained from *Centipeda minimum*. It is a heterocyclic sesquiterpene lactone. Research has shown that Brevilin A has the potential to inhibit cell proliferation, promote cell death, and reduce cell metastasis via lowering the activity of STATS. The researchers, including Lee and Chan, synthesized analogues of Brevilin A to use in their study. In comparison to, the anticancer effects of which were produced from paraformaldehyde and via an aldol reaction with sodium carbonate, were shown to be greater. Drug resistance, systemic toxicity, and ineffective medicines are major issues with cancer treatments. The

complexity of signalling networks and the propensity of most cancer cells to undergo mutations make it very challenging to develop efficient therapeutic agents for the fight against tumors; hence, the rapid discovery of new anticancer agents as drug leads is of the utmost importance. Use of multi-target heterocyclic inhibitors in cancer treatment is one strategy that might address these issues.

That many novel heterocyclic drugs, including Sunitinib (1), Midostaurin (2), and Vorinostat (3), have shown anticancer properties. One of their defining features is their multi-growth factor regulatory capability; this includes VEGFR, c-Kit from PDGFRA, and FLT-3. Phase 3 clinical studies are now underway on a variety of HER1 and HER2 inhibitors, as shown in Figure 1.2. These medicines include sotagliflozin (4), lapatinib (5), erlotinib (6), and gefitinib (7).

MATERIAL AND METHODS

Investigating Novel Non-Estradiol Chemo-Types as Aromatase Inhibitors in a Controlled Environment (5,7)

Due to the high need for new pharmaceutical discoveries, in-silico trials are a proactive way to generate new drug models.

Thanks to in-silico studies conducted by multiple researchers using state-of-the-art tools such as Structure-Guided Design, High-Throughput Docking, and pharmacophore-based modeling approaches, the aromatase enzyme's activity was better understood, and new and powerful artificial intelligences were developed. More sophisticated methods, such as membrane-bound molecular dynamic simulations, have improved our understanding of aromatase's structure and function.

Evidence suggests that the charged amino acid sequence of aromatase—which contains both alkyl and aryl amino acids—is essential for AI interaction. As an electron donor and stabilizer of the substrate's transition state via its oxidation state, heme porphyrin is an essential component of the active site.

For substrate access to the active site channel, the Aspartic acid 309 residue at the entrance to the active site is critical, according to Park et al.'s molecular modeling of the aromatase active site. Another point to note is that when AIs have sp² nitrogen in their heterocyclic structure, the heme-porphyrin complex commonly coordinates the aromatase active site. It was discovered that sixteen separate aromatase mutations occurred at amino acid residues 133, 235, 395, 474, 302, 308, 309, Threonine, Serine 478, and 480. These mutations may significantly alter the ligand binding affinity for aromatase active site amino acid residues.

Creating a QSAR Prototype

To validate the model, we examined at the IC₅₀ activity and chemical variety of the ligands in the aligned training set.

The objective was to come up with useful forecasts. In order to do the regression using a partial least squares (PLS) technique, a number of models were created using four separate PLS tools. The strongest association between the training set and Partial Least Square factors led to the selection of PLS factor 4 (# Factor), which, as shown in Table 3.1, produced the highest levels of statistical significance and overall model significance. With these features, we could evaluate the test set's predictive capability with a Q₂ of 0.7854, RMSE of 0.5284, and Pearson R of 0.9111. F is a variance measure. Greater statistical significance is associated with greater values of F in regressions.

The significance level of the variance ratio is represented by P. With decreasing P values, we can say with more confidence. In order to get the predicted activities' Q-squared value, multiply Q₂ by each one individually. The level of agreement between the predicted and actual activity on the test set is measured by Pearson-R. Prediction 3D QSAR models that fulfilled all of these requirements at once were the most promising. (6)

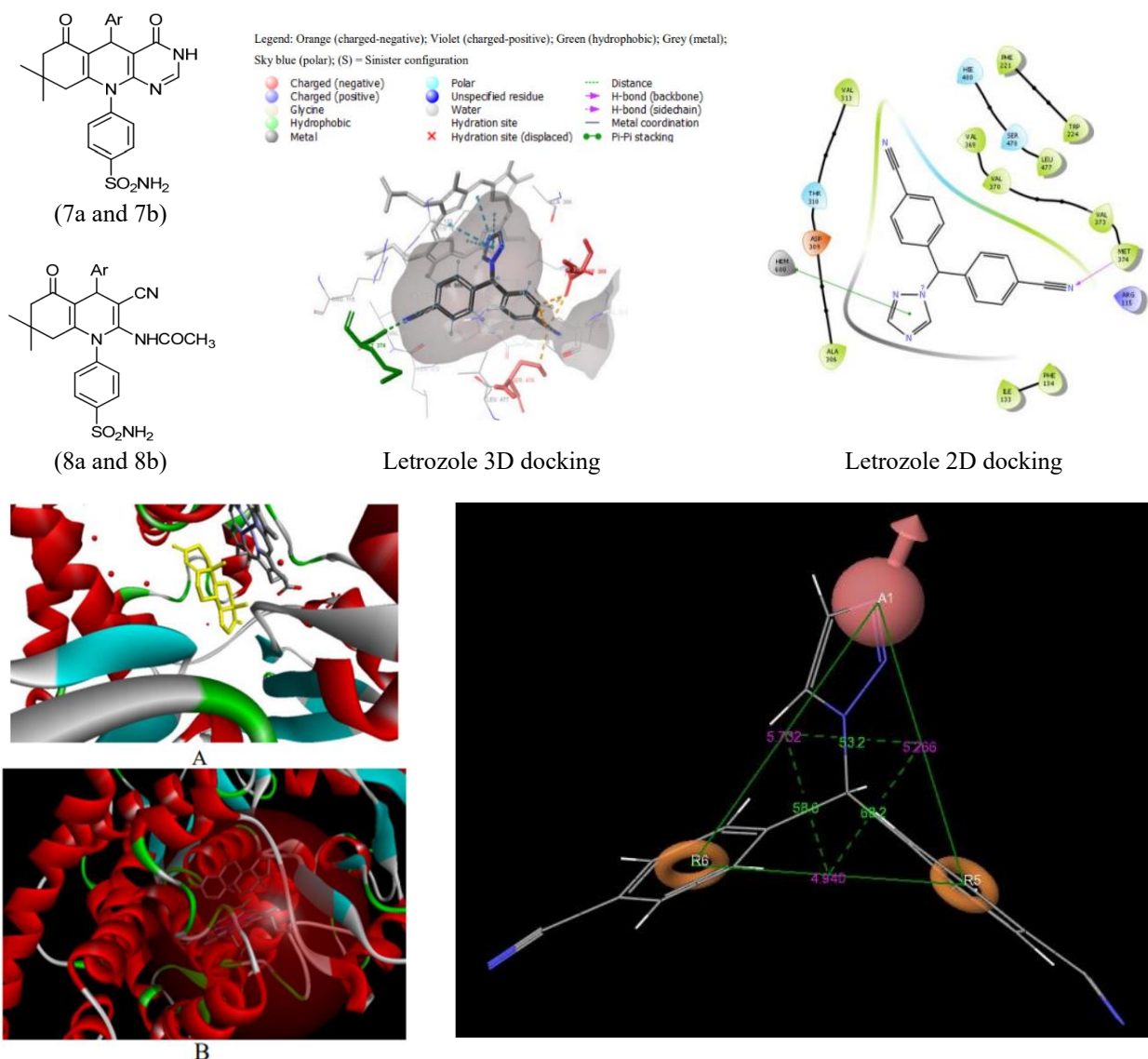


Figure 1: The 3S7S and 3EQM aromatase proteins (A and B)

Figure 2: Potential structure of a pharmacophore

Table 1: Assessment of the best pharmacophore hypothesis ARR.1 using partial Least Squares

S. No.	# Factors	SD	R-Squared	F	P	Stability	RMSE	Q-Squared	Pearson-R
1	1	0.7851	0.5544	27.4	3.014e-005	0.6157	0.8218	0.4809	0.7716
2	2	0.5422	0.7972	41.3	5.313e-008	0.3104	0.6054	0.7183	0.8589
3	3	0.2807	0.9482	122.1	5.006e-013	0.1769	0.5096	0.8003	0.9302
4	4	0.1265	0.99	470.6	1.033e-018	0.094	0.5284	0.7854	0.9111

Table 3: Microanalysis and physical data of molecules 7a and 7b

Compd. No.	Ar	M.p. (°C)	Yield (%)	Mol. Formula (M. wt.)	Microanalysis	
					Calculated	Found
7a	C ₆ H ₄ F-4	168-70	79	C ₂₅ H ₂₃ FN ₄ O ₄ S (494.54)	C: 60.72 H: 4.69 N: 11.33	C: 60.82 H: 4.84 N: 11.49
7b	C ₆ H ₄ Cl-4	162-4	78	C ₂₅ H ₂₃ ClN ₄ O ₄ S (510.99)	C: 58.76 H: 4.54 N: 10.96	C: 58.94 H: 4.38 N: 11.18

Table 2: Analysis of compounds 6a and 6b using microscopy and physical data

Compd. No.	Ar	M.p. (°C)	Yield (%)	Mol. Formula (M. wt.)	Microanalysis	
					Calculated	Found
6a	C ₆ H ₄ F-4	282-4	86	C ₂₄ H ₂₃ FN ₄ O ₃ S (466.53)	C: 61.79 H: 4.97 N: 12.01	C: 61.91 H: 4.73 N: 11.80
6b	C ₆ H ₄ Cl-4	280-2	85	C ₂₄ H ₂₃ ClN ₄ O ₃ S (482.98)	C: 59.68 H: 4.80 N: 11.60	C: 59.92 H: 5.00 N: 11.33

Table 4: Analysis of compounds 8a and 8b using microscopy and physical data

Compd. No.	Ar	M.p. (°C)	Yield (%)	Mol. Formula (M. wt.)	Microanalysis	
					Calculated	Found
8a	C ₆ H ₄ F-4	150-2	97	C ₂₆ H ₂₅ FN ₄ O ₄ S (508.56)	C: 61.40 H: 4.95 N: 11.02	C: 61.68 H: 5.11 N: 10.83
8b	C ₆ H ₄ Cl-4	149-51	82	C ₂₆ H ₂₅ ClN ₄ O ₄ S (525.02)	C: 59.48 H: 4.80 N: 10.67	C: 59.31 H: 5.05 N: 10.49

5-[5-(4-fluorophenyl)-8,8-dimethyl-4,6-dioxo-3,4,6,7,8,9-hexahydro-pyrimido[4,5-b]quinolin-10(5H)-yl] benzenesulfonamide and 4-[5-(4-chlorophenyl)-8,8-dimethyl-4,6-dioxo-3,4,6,7,8,9-hexahydropyrimido[4,5-b]quinolin-10(5H)-yl]isothiocyanate (7b)

After refluxing a solution of compound 6a or 6b (0.001 mol) in 20 ml of formic acid for 5 hours, cooling the mixture, and 7a and 7b were produced when the ensuing solid was crystallised from dioxane after it was ultimately poured into cold water.

1,4,5,6,7,8-hexahydroquinolin-2-yl -[3-Cyano-4-(4-fluorophenyl)-7,7-dimethyl-5-oxo-1-(4-sulfamoyl-phenyl)] Eighthly, acetamide in addition to N-[4-(4-

chlorophenyl)-3- cyano-7,7-dimethyl-5-oxo-1-(4-sulfamoylphenyl)-1,4,5,6,7,8-hexahydroquinolin-2-yl]8-benzoic acid

For the preparation of 8a and 8b, respectively, after a solution of compound 6a or 6b (0.001 mol) was refluxed in 20 ml of acetic anhydride for 5 hours, the reaction mixture was concentrated. The solid that had separated was then crystallised from ethanol. (4,7)

RESULTS

3D QSAR

The ARR three-point pharmacophore model is composed of two aromatic rings (R) and one hydrogen bond acceptor

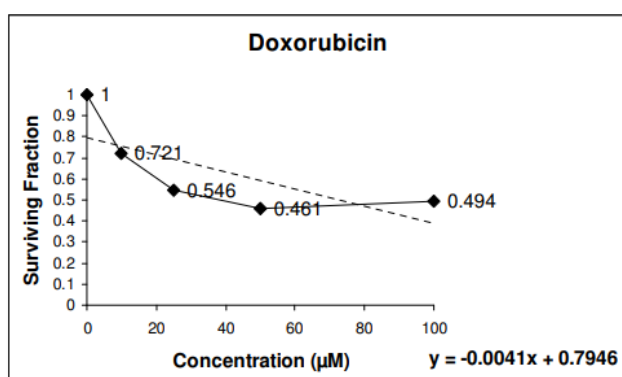


Figure 3: Time to death plot for doxorubicin

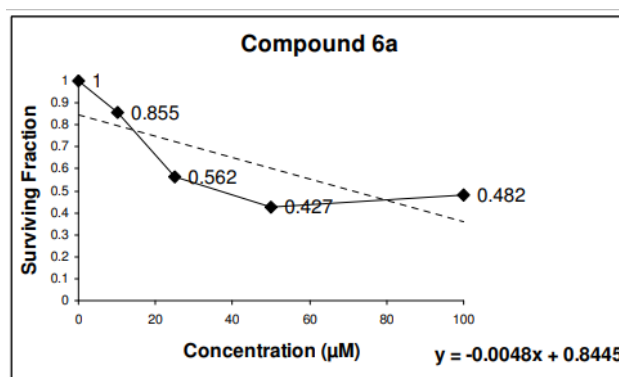


Figure 4: Time required for component 6a to degrade

(A). The 3D-QSAR model successfully predicted the test and training sets' performance using the pharmacophore-based alignment hypothesis.

whether one looks at the 3DQSAR model in the Workspace (Figure 4.8), they can see whether the ligand qualities affect the expected activity positively or negatively. The prototypical form of letrozole is shown by this 3D QSAR model. The blue cubes on the hydrogen bond acceptor region include nitrogen and oxygen, which makes them a suitable location for these atoms to bind, which has a positive impact on biological activity. As the red cubes outside the H-bond acceptor zone demonstrate, biological activity is negatively affected by an environment that is less than perfect for attaching functional groups. A higher vector score indicates that the aligned structures are significantly impacted by vector properties like aromatic rings and acceptors. Every pair of structures gets its volume score from overlapping van der Waals models of non-hydrogen atoms. The presence of a hydrogen bond acceptor (A), which might be oxygen or nitrogen, is necessary to enhance the ligand's effectiveness.

Docking Results

Using the Glide XP Visualiser in the maestro workspace, we built the active site surface mesh to improve the interactions between receptors and ligands. Aromatase receptor site shape is one of the fascinating new findings. It looks like a regular iodine flask. The hydrophobic active site contains L-phenylalanine 221 and L-Valine 313 at its conical entrance. Essential for aromatization, the heme prosthetic group (gray) forms the flat base of the flask and supplies electrons to the substrate. (Letrozole 3D and 2D docking)

Biological Activity

In-vitro Anticancer Screening

It was the National Cancer Institute's pharmacology department at Cairo University that conducted the *in vitro* anticancer screening. This research used the MCF7 cell line, which is a human malignancy breast cell line. Using the Sulfo-Rhodamine-B stain (SRB) test, which was developed by Skehan et al., the cytotoxic activity of the newly synthesized compounds was assessed *in vitro*. Since its introduction in 1990, the SRB test has been one of the most used methods for *in vitro* cytotoxic screening. Here, we use tissue-culture plates to test SRB's binding affinity for cell protein components fixed with trichloroacetic acid (TCA). The vibrant pink aminoxanthene dye SRB binds to basic amino acid residues in slightly acidic environments but dissociates in basic ones. Two sulfonic groups are included in the dye. Cells were seeded onto a 96-well plate at a density of 10 4 cells/well and left to adhere to the plate wall for 24 hours prior to being treated with the compound(s) under study. Three independent wells were dug for each concentration. The substance(s) was/were allowed to incubate with the cells for 48 hours at 37 °C in a 5% CO₂ setting. Fixation, washing, and staining with a solution containing 0.4% (wt/vol) SRB in 1% acetic acid were performed on the cells after 48 hours. To remove the excess unbound color, four washes with 1% acetic acid were necessary. Tris-EDTA buffer was then used to assist restore the attached stain. An

Table 5: Novel chemotypes' 3D QSAR findings (compound 35-66)

S.No.	Ligand	Predicted Activity	Align Score	Vector Score	Volume Score	Fitness
1	35	0.8697	0.043914	0.923434	0.553571	2.440411
2	36	-0.80296	0.256423	0.784339	0.442922	2.013576
3	37	-0.80296	0.2564	0.784376	0.454333	2.025042
4	38	-0.80296	0.256671	0.784165	0.457547	2.02782
5	39	-0.80296	0.256245	0.78448	0.456471	2.027413
6	40	0.737991	0.044625	0.923212	0.425	2.311024
7	41	0.852453	0.043946	0.923415	0.563636	2.450429
8	42	-0.73642	0.256497	0.784367	0.464115	2.034734
9	43	-0.73642	0.25638	0.784372	0.460808	2.03153
10	44	-0.70664	0.277472	0.772249	0.478673	2.019696
11	45	0.800144	0.277472	0.772249	0.478673	2.019696
12	46	-0.7974	0.043947	0.92334	0.570552	2.457269
13	47	-0.7974	0.25642	0.784365	0.468599	2.03928
14	48	-0.7974	0.256828	0.784019	0.454333	2.024329
15	49	-0.76701	0.256095	0.784621	0.465228	2.036436
16	50	0.965794	0.428475	0.805351	0.5075	1.955788
17	51	-0.47892	0.066766	0.949119	0.566265	2.459746
18	52	-0.81155	0.407089	0.839301	0.453488	1.953549
19	53	-0.69853	0.407735	0.839245	0.447005	1.946471
20	54	-0.59219	0.40921	0.839001	0.450935	1.948927
21	55	0.633341	0.406863	0.834213	0.44213	1.93729
22	56	-0.66154	0.066775	0.9491	0.583851	2.477305
23	57	-0.654	0.417373	0.760761	0.459135	1.872085
24	58	-0.654	0.407764	0.839176	0.455399	1.954771
25	59	-0.654	0.407765	0.839127	0.46747	1.966792
26	60	0.791436	0.4078	0.839162	0.472019	1.971348
27	61	0.767623	0.044013	0.923331	0.561934	2.448587
28	62	-0.61032	0.066866	0.949051	0.582043	2.475373

ELISA reader detected the strength of the colors at a wavelength of 570 nm.

CONCLUSION

Recent developments in the synthesis of heterocyclic ring-containing compounds with anticancer properties, particularly in the development of target-based anticancer medications, have been the major focus of this research. Like other treatments, anticancer drugs include heterocyclic moieties that improve their pharmacokinetic and pharmacodynamic properties. Roughly 30% of the anticancer drugs approved by the FDA include one or more heterocyclic rings that consist of sulfur, nitrogen, and oxygen. Heterocyclic moieties play an important role in several metabolic processes that are necessary for all living things to function. Their pivotal role in cancer research and the fight against cancer was shown by the fact that they were incorporated in about two-thirds of the anticancer drugs authorized by the FDA in the first half of the decade. These efforts have also centred on developing new methods for using heterocyclic chemicals as anticancer medications, which has recently seen significant progress.

REFERENCES

1. Mirza, Agha Zeeshan. (2019). Advancement in the development of heterocyclic nucleosides for the treatment of cancer - A review. *Nucleosides, Nucleotides and Nucleic Acids*. 38. 1-22. 10.1080/15257770.2019.1615623.
2. Naturalista, & Issn, & Panda, Krishna. (2024). Exploring the Synthetic Strategies and Biological Activities of Pyrazole Derivatives. 2024.
3. Didehban, Khadijeh & Vessally, E. & Salary, Mina & Edjlali, Ladan & Babazadeh, Mirzaagha. (2018).

- Synthesis of a variety of key medicinal heterocyclic compounds via chemical fixation of CO₂ onto o-alkynylaniline derivatives. *Journal of CO₂ Utilization*. 23. 42-50. 10.1016/j.jcou.2017.10.025.
4. Martins, Pedro & Jesus, João & Santos, Sofia & Raposo, Luís & Rodrigues, Catarina & Baptista, Pedro & Fernandes, Alexandra. (2015). Heterocyclic Anticancer Compounds: Recent Advances and the Paradigm Shift towards the Use of Nanomedicine's Tool Box. *Molecules* (Basel, Switzerland). 20. 16852-16891. 10.3390/molecules200916852.
 5. Ledade, Pankaj & Lambat, Trimurti & Gunjate, Jitendra & Chopra, P.K.P. & Bhute, Amitkumar & Lanjewar, Mamata & Kadu, Pooja & Dongre, Utpal & Mahmood, Sami. (2022). Nitrogen-containing Fused Heterocycles: Organic Synthesis and Applications as Potential Anticancer Agents. *Current Organic Chemistry*. 27. 10.2174/1385272827666221227120648.
 6. Kumar, Naresh & Goel, Nidhi. (2022). Heterocyclic Compounds: Importance in Anticancer Drug Discovery. *Anti-Cancer Agents in Medicinal Chemistry*. 22. 10.2174/1871520622666220404082648.
 7. Sapra, Ritu & Dhara, Patel & Meshram, Dhananjay. (2019). A mini review: recent developments of heterocyclic chemistry in some drug discovery scaffolds synthesis. 3. 71-78. 10.26655/JMCHEMSCI.2020.1.9.